The potential of local climate zones maps as a heat stress assessment tool, supported by simulated air temperature data

Marie-Leen Verdonck[a,*], Matthias Demuzere[a], Hans Hooyberghs[b], Christoph Beck[c], Josef Cyrys[d], Alexandra Schneider[d], Robert Dewulf[a], Frieke Van Coillie[a]

[a] Department of Environment, University Gent, Belgium
[b] Vlaamse Instelling voor Technologisch Onderzoek (VITO), Belgium
[c] Institute for Geography, University of Augsburg, Germany
[d] Institute of Epidemiology II, Helmholtz Zentrum München – German Research Center for Environmental Health (GmbH), Germany

ARTICLE INFO

Keywords:
Urban heat islands
Local climate zones
Thermal behaviour
Heat stress
Belgium
UrbClim model

ABSTRACT

High population densities in cities and rapid urban growth increase the vulnerability of the urban environment to extreme weather events. Urban planning should account for these extreme events as efficiently as possible. One way is to locate hot spots in an urban environment by mapping cities into local climate zones (LCZ) and evaluate heat stress related to these zones. LCZs are likely to become a standard in urban climate modelling as they capture important urban morphological characteristics. For instance, temperature regimes linked to spatially explicit LCZ maps should be assessed for all LCZ zones derived from these maps. This study assesses the thermal behavior of mapped LCZs using simulated temperature data from the UrbClim model. Prior to temperature analysis, the model was validated with observational data. To evaluate the robustness of the analysis, we ran the model in three cities in Belgium: Antwerp, Brussels, and Ghent. The results show that temperature regimes are significantly different for all the built zones in the urban environment independent of the city. Second, the susceptibility to heat stress can differ greatly depending on the zone. The unique thermal behavior of the different LCZs provides indispensable information on the urban environment and its climatic conditions. This study shows that the LCZ scheme has a potential to help urban planners globally tackle adverse effects of extreme weather events.

1. Introduction

As Earth's climate continues to change over the coming decades, global warming will hit urban centers especially hard. This poses a major threat to the health and well-being of urban human populations (Hoag, 2015). At the same time, urban centers are facing problems associated with high levels of anthropogenic emissions, resulting from e.g. residential energy or increased traffic, potentially leading to premature mortality globally (Lelieveld, Evans, Fnais, Giannadaki, & Pozzer, 2015; Solberg et al., 2008) and are subject to an increase in impervious and built surfaces, which can significantly alter the local climate (Papalexiou, AghaKouchak, Trenberth, & Foufoula-Georgiou, 2018; Sundborg, 1951). Even though climate change and the alteration of local climate take place on different spatial scales, global warming can intensify the effects on local climate in the urban areas due to a phenomenon called urban heat islands (UHI), causing large air temperature differences between urban and surrounding rural sites (Oke, 1976). The higher frequency of severe heatwaves, in combination with the UHI effect, has a compounding effect on thermal conditions in urban areas. (Barriopedro, Fischer, Luterbacher, Trigo, & Garcia-Herrera, 2011; Grimm et al., 2008; Hoag, 2015; Lauwaet, Maiheu, Aertsens, & De Ridder, 2013; Maiheu, Van den Berghe, Boelens, De Ridder, & Lauwaet, 2013; Schär et al., 2004; Wouters et al., 2017).

Currently, 54% of the global population lives in cities, which cover only 3% of the Earth's land surface (Mills, 2007). Projections show that the proportion of global population living in urban areas will increase to 70% by 2050 (UN, 2014). The increasing urban population and quickly rising global temperatures will put additional pressure on cities, resulting in unhealthy living conditions (Aertsens et al., 2012; WMO, 2013). In the past decades more than 120,000 people have died due to extreme heat in Europe and Russia, 75% of which occurred in cities (WMO, 2013); Many thousands more were exposed to heat stress. Heat

* Corresponding author at: Coupure 653, B-9000 Gent, Belgium.
E-mail addresses: marieleen.verdonck@ugent.be (M.-L. Verdonck), matthias.demuzere@ugent.be (M. Demuzere), hans.hooyberghs@vito.be (H. Hooyberghs), Christoph.beck@geo.uni-augsburg.de (C. Beck), cyrys@helmholtz-muenchen.de (J. Cyrys), alexandra.schneider@helmholtz-muenchen.de (A. Schneider), robert.dewulf@ugent.be (R. Dewulf), frieke.vancoillie@ugent.be (F. Van Coillie).

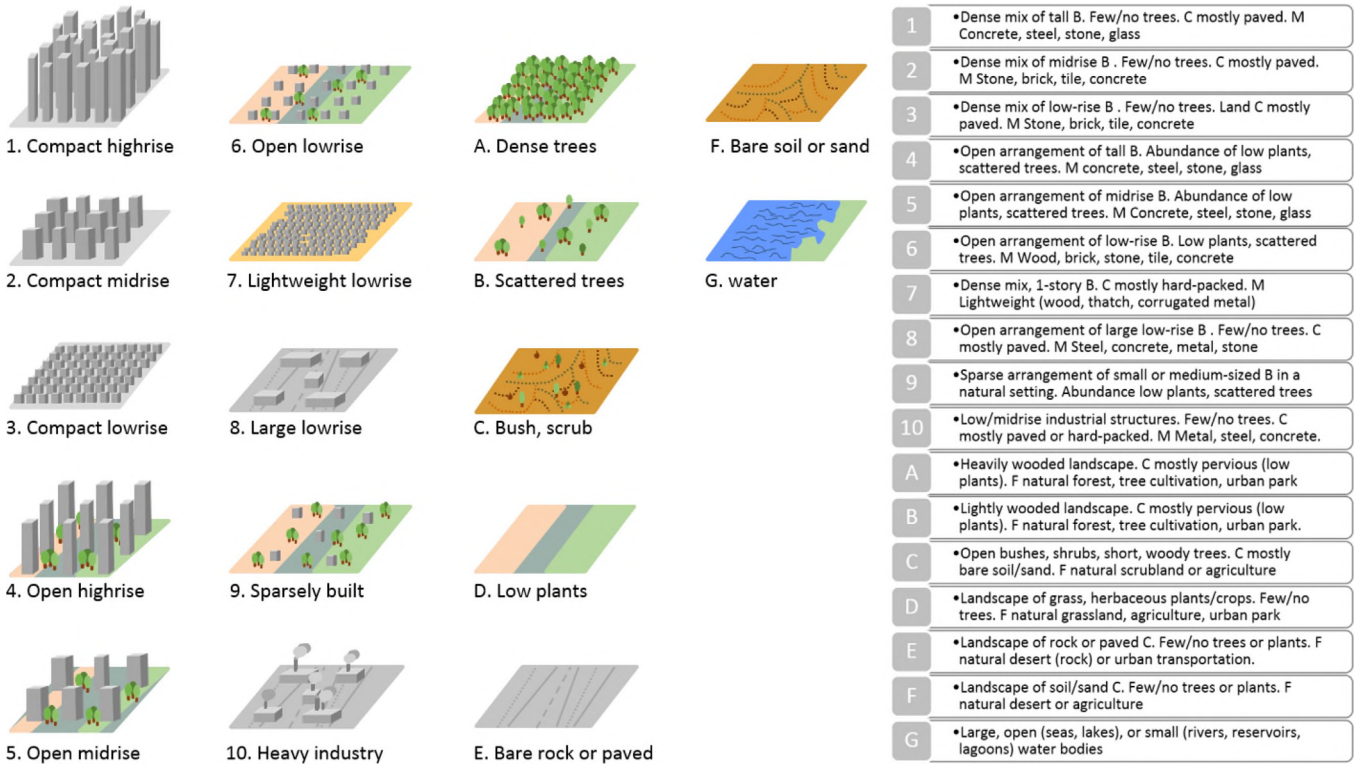

Fig. 1. Urban (1–10) and natural (A–G) LCZ types and their characteristics (adapted from Table 2 in (Stewart & Oke, 2012), text shortened, icons reworked) B: Buildings; C: cover; M: materials; F: function; Tall: > 10 stories, Midrise: 3–9 stories, Low: 1–3 stories (Adapted from Stewart & Oke, 2012).

stress occurs when the human body's means of regulating its internal temperature starts to fail (Werder, 2010). This failure can affect physiological processes and result in various strains on the body (e.g. dehydration). A 3 °C increase in internal temperatures within the human body can be lethal (Simon, Niiro, & Gwinn, 1993). Recently, Mora et al. (2017) argued that 30% of the world's population is exposed to climate conditions that lead to lethal heat events, a number that is expected to increase to 74% under the projected growing greenhouse gas emissions. In the face of these threats, knowledge of critical areas should be made available and urban planners should consider the health issues arising from the urban climate when developing new projects (Koppe, Kovats, Jendritzky, & Menne, 2004). It is therefore necessary to introduce supporting research on areas most susceptible to heat stress (Koppe et al., 2004; Pickett, Cadenasso, & McGrath, 2013).

There are three primary ways to counteract the unwanted effects of urban heat (Rizwan, Dennis, & Liu, 2008): (1) reducing anthropogenic heat release; (2) climate sensitive roof design; (3) other design factors. The first method mainly focusses on reducing air conditioning and other urban or building design factors (Kikegawa, Genchi, Kondo, & Hanaki, 2006; Urano, Ichinose, & Hanaki, 1999; Yamamoto, 2005). Climate sensitive roof design includes measures such as green and reflective roofs as well as roof spray-cooling (Jain & Rao, 1974; Rosenfeld, Akbari, & Romm, 1998; Takebayashi & Moriyama, 2007). Finally, other design factors can include the introduction of more vegetation and water, urban ventilation, the use of high reflective building materials, and the general increase in albedo (Aertsens et al., 2012; Bowler, Buyung-Ali, Knight, & Pullin, 2010; Coutts, Tapper, Beringer, Loughnan, & Demuzere, 2012; Demuzere et al., 2014; Feyisa, Dons, & Meilby, 2014; Rizwan et al., 2008; Salmond et al., 2016; Sun & Chen, 2012; Weng, Lu, & Schbring, 2004). In addition to these well-known adaptation and mitigation strategies, adjusting urban morphology can have a major effect on the thermal behaviour of a city due to better ventilation, lower heat absorption, and increased evaporation. Simple tools for relating urban morphology to possible heat stress are thus of high interest for urban planners (Heldens, Taubenböck, Esch, Heiden, & Wurm, 2013; IPCC., 2018; Kleerekoper, Van Esch, & Salcedo, 2012; Shahmohamadi, Che-Ani, Maulud, Tawil, & Abdullah, 2011).

Various models, operating on different scales, can be used to assess the urban climate depending on the aim of the study and the surface of the study area (Best & Grimmond, 2015; Mirzaei, 2015; Toparlar, Blocken, Maiheu, & van Heijst, 2017). As this study focuses on neighborhood-scale urban heat island dynamics, the UrbClim model is used; a simple urban surface energy balance model designed to target the spatial scale of an urban agglomeration yet fast enough to allow integrations over multiple summer seasons while maintaining a satisfactory level of accuracy (De Ridder, Lauwaet, & Maiheu, 2015; García-Díez et al., 2016). The scheme was developed from an existing land-surface scheme adapted to urban surfaces (De Ridder, 2006; Demuzere, De Ridder, & Van Lipzig, 2008), and can be classified as a slab surface (type L1) land surface model (Grimmond et al., 2011). Similar to most other urban land surface schemes (for a non-comprehensive overview see e.g. Best and Grimmond (2015)), one need to accurately describe the urban land surface, as modelled temperatures and urban energy balance components are known to be sensitive to the urban canopy parameters used (Demuzere et al., 2017; Grimmond et al., 2011; Wouters et al., 2016). Ideally, spatial site-specific information is available, yet often generalized global values are used to describe the morphological, radiative and thermal properties of the impervious surfaces, such as the Jackson, Feddema, Oleson, Bonan, and Bauer (2010) database and the ECOCLIMAP data (Champeaux, Masson, & Chauvin, 2005; Faroux et al., 2013). Since the introduction of 'Local Climate Zone' concept by Stewart and Oke (2012), progress has been made to integrate these structural and land cover classes and related generic urban canopy properties into urban canopy schemes (Alexander, Fealy, & Mills, 2016; Brousse, Martilli, Foley, Mills, & Bechtel, 2016; Hammerberg, Brousse, Martilli, & Mahdavi, 2018; Stewart, Oke, & Krayenhoff, 2014; Wouters et al., 2016). The Local Climate Zone classification scheme was originally developed to ease comparison of observational urban heat island (UHI) studies and to provide an objective protocol for measuring the UHI intensity. The

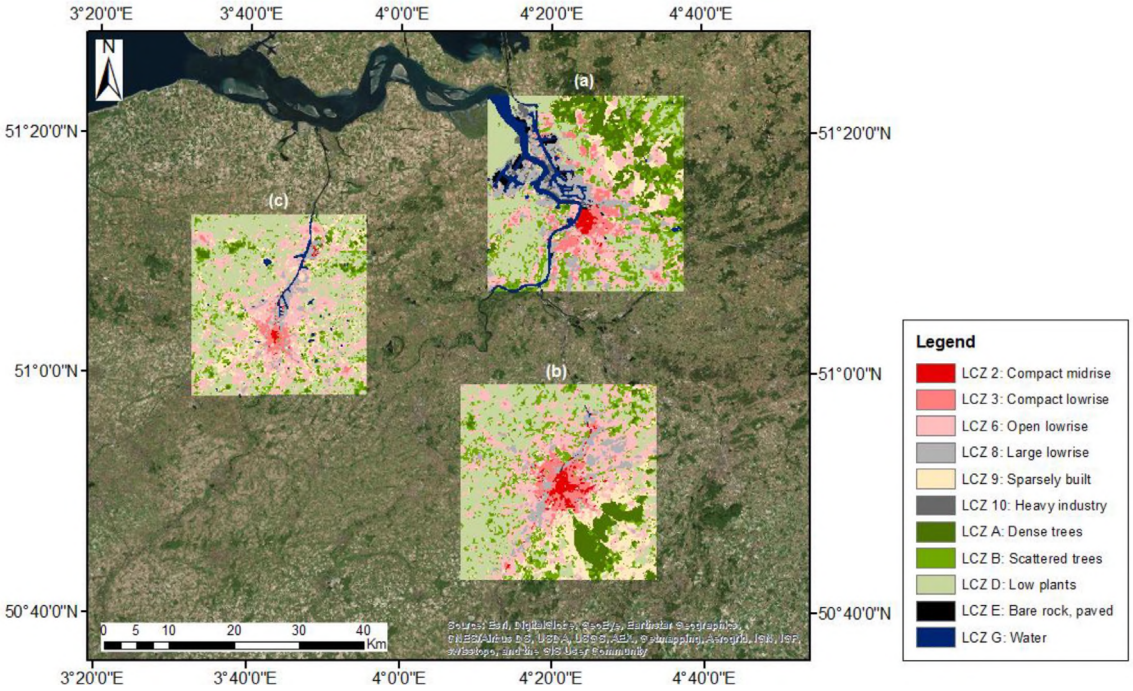

Fig. 2. Antwerp (a), Brussels (b) and Ghent (c) (basemap © ESRI; a larger version of the LCZ maps is available in Verdonck et al. (2017)).

zones are formally defined as: "regions of uniform surface cover, structure, material, and human activity that span hundreds of meters to several kilometers in horizontal scale" (Stewart & Oke, 2012). The scheme consists of 17 standard LCZs, with a unique air temperature regime at screen height (1–2 m above ground) and in similar atmospheric and surface relief conditions (Stewart et al., 2014) (Fig. 1).

Following the development of LCZs, a method was presented by Bechtel et al., (2015), within the World Urban Database and Access Portal Tools (WUDAPT) initiative, to classify urban areas into spatially explicit LCZ maps. Recently, an adaptation of this method was published by Verdonck et al., (2017) to classify small heterogeneous cities that resulted in high accuracy maps. Even though the mapping of LCZs is not the primary goal of the scheme, many people all over the world are adapting LCZs to that purpose (Ching et al., 2018; WUDAPT, n.d.). The logical structure of the LCZ classification scheme is supported by observational and numerical modelling data to determine specific thermal characteristics for each zone (Stewart et al., 2014). Since the launch of the LCZ scheme, many studies have been performed analyzing the thermal behavior of specific locations with measurement equipment in different LCZs (Leconte, Bouyer, Claverie, & Pétrissans, 2017; Lehnert, Geletič, Husák, & Vysoudil, 2014; Puliafito, Bochaca, Allende, & Fernandez, 2013). Other studies have analyzed the intra-urban temperature differences by combining LCZ-maps with stationary and mobile measurements (Alexander & Mills, 2014; Fenner, Meier, Bechtel, Otto, & Scherer, 2017; Holmer, Thorsson, & Lindén, 2013; Kotharkar & Bagade, 2018; Ndetto & Matzarakis, 2015; Skarbit, Stewart, Unger, & Gál, 2017; Thomas, Sherin, Ansar, & Zachariah, 2014; Villadiego & Velay-Dabat, 2014). From these studies, we can conclude that the LCZ scheme can play an important role in UHI evaluation. However, none of the studies that use LCZ maps for thermal evaluation of the LCZ scheme have reported on the accuracy of these maps. It has been shown that highly accurate maps are required to evaluate thermal behavior (Verdonck et al., 2017) and that maps for which accuracy is only based on visual interpretation often do not meet this requirement (Bechtel et al., 2017).

Until now, it remained unclear whether neighborhood scale urban climate models could accurately simulate the thermal characteristics present in the LCZs. In this study, we investigate the thermal characteristics of LCZ maps in European cities using spatially explicit, simulated air temperature data. Moreover, we evaluated the usability of LCZ maps as an objective indicator for heat stress. The combined use of spatially explicit air temperature evaluation and heat stress analysis can provide urban planners with much needed information on urban hot spots. The use of modelled air temperature requires a thorough evaluation of the model. For this study, we used the UrbClim model (De Ridder et al., 2015) to analyze the thermal characteristics in the different LCZs for three study sites in Belgium. The three study sites were chosen to evaluate the robustness of the presented results in one of the most densely populated and urbanized areas in Europe (The World Bank, 2017). The model can operate at a high spatial and temporal resolution (100 m and 1 h, respectively) over a study area around 30 by 30 km. With these parameters, the dynamic nature of the UHI can be examined. The 100 m resolution allows one to assess the intra-urban temperature differences between different neighborhoods in cities. The local scale of the model creates opportunities to differentiate between temperature regimes in the urban environment with respect to morphologically distinct neighborhoods.

The main objective of this study is to evaluate whether LCZ maps can serve as a tool for heat stress assessment. To that end, three sub-objectives are outlined: i) evaluate the performance of the UrbClim model in relation to the observed thermal differentiation between the LCZs, ii) verify the robustness of the thermal behavior of LCZs using LCZ maps for the three biggest urban areas in Belgium and iii) assess the use of LCZs as an objective indicator for heat stress on hot days.

2. Data and methods

2.1. Study area

In this study, we focus on the three largest urban areas in Belgium, different in population numbers and densities: Antwerp (surface area (SA) = 204.5 km^2, population (pop) = 500,000), Brussels (SA = 161.4 km^2, pop = 1200,000) and Ghent (SA = 156.2 km^2, pop = 250,000) (Fig. 2). Flanders and the Brussels capital region are located a mid-latitude maritime climate regime and topographically the study areas are located in the flatlands of Northern Belgium. Both

Antwerp and Ghent are characterized by large harbor areas in the North. While Brussels does not have heavy industry, it contains a large commercial zone with low intensity industry along the canal, which crosses the city from South West to North East. The South Eastern part of Brussels is dominated by a large forested area: The Sonian forest.

For all of the areas, grids of 30 by 30 km around the city center, were defined and LCZ maps were available at a resolution of 100 m based on the method proposed by Verdonck et al. (2017). The method extends the default LCZ mapping methodology from Bechtel et al. (2015) by using neighborhood information in the classification procedure. This was shown to be highly effective for the Belgian heterogeneous cities, resulting in a significant improvement of the accuracy of the LCZ maps (Fig. 2). For more details on the procedure, we refer to Verdonck et al. (2017). The LCZ maps show that the three study sites are characterized by a compact medieval core dominated by compact mid and lowrise zones (LCZ 2 & LCZ 3) surrounded by urban sprawl, characterized by open low rise and sparsely built zones (LCZ 6 & LCZ 9). Since Ghent is the smallest of the three study sites, compact midrise or LCZ 2 is less abundant compared to the other cities.

None of the urban areas of interest in this study have sufficient air temperature data available across the existing LCZs to validate the performance of the UrbClim model. To assess thermal characteristics between simulated and measured ambient air temperature, we selected the city of Augsburg in Bavaria, Southern Germany. Augsburg is a small city (SA = 146.84 km^2, pop = 290,000), characterized by a humid continental climate and situated at the convergence of the Alpine rivers Lech, Wertach and Singold. Since 2014, 80 loggers have measured air temperature in Augsburg, providing much needed data to validate simulated air temperature (see also Section 2.3) (Fig. 3). A LCZ map for the city of Augsburg was developed using the same method outlined in Verdonck et al. (2017), resulting in an overall accuracy of 92.8% (Fig. A1). Augsburg is also characterized by a medieval core dominated by compact midrise zones (LCZ 2) surrounded by urban sprawl, characterized by open mid and lowrise zones (LCZ 5 & LCZ 6). The temperature data from the city of Augsburg is used to assess whether the UrbClim model is able to thermally distinguish between the different LCZs. Thereafter, assessment of the thermal behavior and heat stress in the LCZs is based on the model runs over the Belgian cities (Fig. 4).

2.2. UrbClim model

2.2.1. Model description

The UrbClim model is based on a soil-vegetation atmosphere transfer scheme, named the Land Surface Interaction Calculation (LAIca) (De Ridder & Schayes, 1997), which was expanded in recent years to account for urban surfaces (De Ridder et al., 2015). This scheme calculates the heat fluxes at the surface based on the surface energy balance. The surface is divided in grid cells, which are all composed of fractions of vegetation, bare soil, and urban surface. Each grid cell features its own energy balance and corresponding thermal behavior. The urban surface is presented as a rough impermeable area characterized by several land use related parameters (albedo, emissivity, roughness length, stomatal and total plant resistance, root distribution coefficient, and soil sealing). For each of the three land cover types separate energy and water balances are considered. The soil-vegetation atmosphere transfer scheme is coupled to a 3-D atmospheric module, which includes the atmospheric boundary layer and extends to a height of three kilometers. The default version of the UrbClim model has been validated for several European cities, for example for Antwerp, Brussels and Ghent (Belgium), Toulouse (France) and Barcelona (Spain) (De Ridder et al., 2015; García-Díez et al., 2016; Lauwaet et al., 2015, 2016).

2.2.2. Data inputs and outputs

Large-scale meteorological information is considered by including data from global or meteorological models. The current study uses ERA-Interim reanalysis data of the European Centre for Medium-Range Weather Forecasts (ECMWF) (Dee et al., 2011). The most important terrain classification input are land use, urban soil sealing, Normalized Differenced Vegetation Index (NDVI), and terrain elevation. A raster cell is determined to be urban or non-urban based on the land use data. In the former case, the grid cell comprises an urban, vegetation and bare soil part. The soil sealing value determines the fraction of built-up zones in the grid cell, and the NDVI determines the fraction of

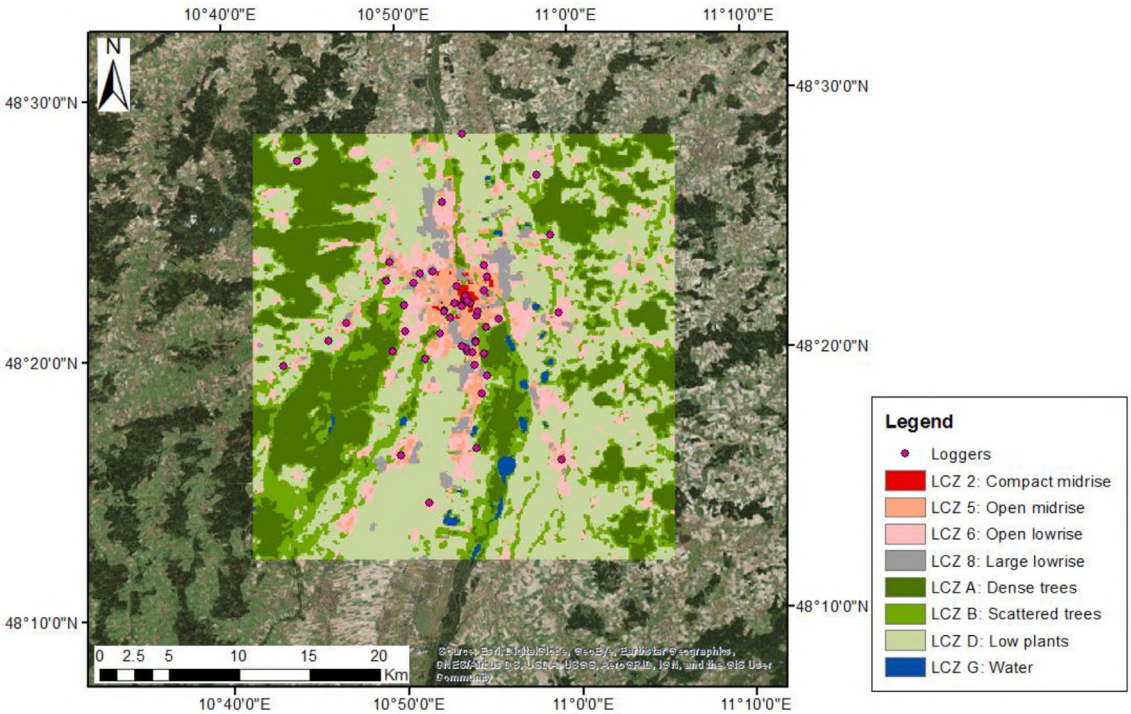

Fig. 3. Observation locations (50) and LCZ map for Augsburg, Germany (basemap © ESRI).

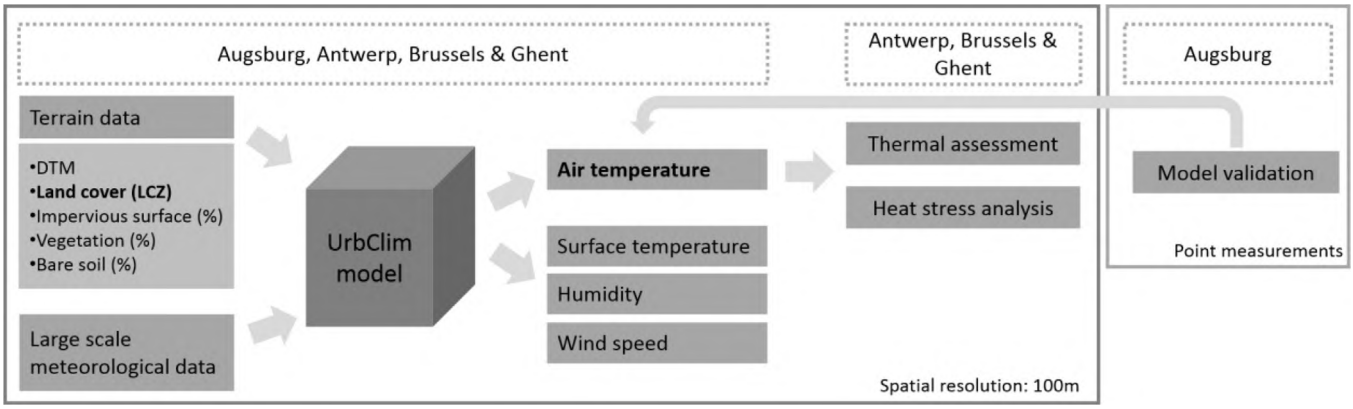

Fig. 4. Workflow including model inputs, outputs, model evaluation of air temperature and an analysis of the thermal behaviour and heat stress related to LCZ's.

vegetation in the cell. In order to take vegetation phenology into account, the NDVI maps vary on a monthly basis. The bare soil fraction is calculated as a complementary fraction when the two fractions do not add up to 100%. For non-urban surfaces only the fraction of vegetation and bare soil is determined.

By default the land cover input is based on the CORINE land cover data for Europe (EEA, 1994), and the soil sealing data originates from the Imperviousness Degree (IMD) data set of the EEA (EEA, 2012). Given the dataset's geographical limitation (European Union) and that the most recent versions of CORINE and IMD date back to 2012, there is a need for other input datasets. We decided to use LCZ maps as a proxy for land cover in our study due to its global applicability. However, the CORINE-based model runs have been extensively validated for the Belgian study areas and for the remainder of this manuscript they are referred to as "the validated model runs" (Lauwaet et al., 2016, 2013; Maiheu et al., 2013).

When using the LCZ maps, grid cells with classes LCZ 1 to LCZ 10 are classified as urban. The urban soil sealing raster data, and thus the fraction of built-up area in the urban grid cells, are based on the sum of the mean building surface fraction and the mean impervious surface fraction in the LCZ fact sheets for each zone in the LCZ map (Stewart & Oke, 2012). Values for albedo, emissivity, thermal conductivity, volumetric heat capacity, aerodynamic and thermal roughness length are assigned to every grid cell based on the land cover data: for each LCZ class we have determined a fixed value for each of these parameters (Table 1) (Stewart & Oke, 2012), and assigned this value to all the grid cells with the corresponding land use.

Finally, terrain elevation data are used from the global GMTED2010 Dataset for all runs (Danielson & Gesch, 2011). For more information on the model specification refer to De Ridder et al. (2015).

UrbClim outputs information on surface and two meter air temperature, near-surface humidity, and wind speed. In this study, only air temperature results have been assessed.

2.3. Meteorological observations

To assess whether the model is able to thermally differentiate between the different mapped LCZs, we compared observations from the city of Augsburg to simulated air temperature from the UrbClim model. Measurements of air temperature and relative humidity are available for the urban area and the rural surroundings of Augsburg, with four minute temporal resolution for 80 sites (temporal data coverage varies among sites) (Beck et al., 2015). We used ONSET HOBO Pro v2 loggers U23-001 (Onset, 2010). According to the manufacturer, the loggers' accuracy for air temperature measurements is ± 0.21 °C from 0° to 50 °C and the respective resolution is 0.02 °C at 25 °C (Onset, 2010). All loggers are located between approximately 1.5 and 2.3 m height above ground. For practical reasons, we were unable to maintain a standard measurement height of 2 m at all sites. The loggers are not ventilated but are equipped with a solar radiation shields. The network is operated and maintained by the Institute of Geography at the University of Augsburg in cooperation with the German Research Center for Environmental Health, Helmholtz Zentrum München (Institute of Epidemiology, Environmental Risks). The logger data are downloaded and the sensors are checked for functionality every two months by a student assistant and a technician. The temperature data are checked every two months for obvious errors (outliers, missing data) by a data manager. Irregularly, the temperature data are quality checked more thoroughly including a fixed range test, tests for temporal as well as spatial outliers, a persistence test and a step test. Due to the fact that the network grew over the last four years, a simultaneous cross calibration of the loggers was not feasible.

Unfortunately, some of the loggers were placed on the edge of several LCZs and cannot be used to analyze the thermal characteristics of the zones individually. After close inspection of the LCZ map and based on expert knowledge of the area, 50 loggers were determined to be representative for their respective LCZ. In Fig. 5, representative logger locations in the different built zones are listed.

The loggers have been measuring air temperature since 2014. However not all loggers were active throughout the whole period. In spite of this, a large set of air temperature records was compiled and a unique experiment was done: the analysis of night-time temperatures based on 50 logger locations (Fig. 3) in different LCZs for the summer months June, July and August of 2014 and 2015. Since the loggers are mainly located in the urban environment, only the thermal characteristics in the urban zones in Augsburg are evaluated in this manuscript (LCZ 2, LCZ 5, LCZ 6 and LCZ 8).

2.4. Assessment strategy

2.4.1. Assessment of the UrbClim model based on Augsburg data

To assess thermal differences between zones, the simulated and observed data are rescaled to unity [0-1], where x is an original value and, x' is the normalized value, in order to facilitate comparison for days with different maximum day-time temperatures.

$$x' = \frac{x - min(x)}{max(x) - min(x)}$$

A statistical t-test was performed to evaluate whether the different LCZs feature significantly different thermal characteristics under clear UHI conditions at night (1 am local time). The significance threshold was set at 0.05. Clear UHI conditions are defined based on two separate terms. First, the data set is filtered for nights with low wind speed and, no rainfall or cloud cover. Second, based on simulated temperature differences over time between the coolest (min) and the warmest (max) zone, days that are characterized by a steep increase in temperature

Table 1
Parameter list for UrbClim run using LCZ maps (based on Stewart & Oke, 2012).

	Vegetation albedo	Soil albedo	Vegetation emissivity	Soil emissivity	Roughness length (m)	Stomatal resistance (s/m)	Total plant resistance (s)	Root distribution coefficient	Soil sealing (%)
LCZ 1: Compact high rise	0.15	0.12	0.98	0.95	2	200	1.00E+09	0.961	1
LCZ 2: Compact mid rise	0.15	0.12	0.98	0.95	0.75	200	1.00E+09	0.961	1
LCZ 3: Compact low rise	0.15	0.12	0.98	0.95	0.5	200	1.00E+09	0.961	0.9
LCZ 4: Open high rise	0.15	0.15	0.98	0.95	1.5	200	1.00E+09	0.961	0.6
LCZ 5: Open mid rise	0.15	0.15	0.98	0.95	0.33	200	1.00E+09	0.961	0.5
LCZ 6: Open low rise	0.15	0.15	0.98	0.95	0.33	200	1.00E+09	0.961	0.4
LCZ 7: Lightweight low rise	0.15	0.12	0.98	0.95	0.15	200	1.00E+09	0.961	0.85
LCZ 8: Large low rise	0.15	0.15	0.98	0.95	0.25	200	1.00E+09	0.961	0.95
LCZ 9: Sparsely built	0.15	0.15	0.98	0.95	0.25	200	1.00E+09	0.961	0.25
LCZ 10: Heavy industry	0.15	0.15	0.98	0.95	0.5	200	1.00E+09	0.961	0.9
LCZ A: Dense trees	0.15	0.15	0.98	0.98	2	200	1.00E+09	0.961	0
LCZ B: Scattered trees	0.15	0.15	0.98	0.98	0.33	200	1.00E+09	0.961	0.05
LCZ C: Bush, scrub	0.15	0.15	0.98	0.98	0.1	200	1.00E+09	0.961	0
LCZ D: Low plants	0.2	0.15	0.98	0.98	0.1	100	5.00E+08	0.961	0
LCZ E: Bare rock or paved	0.2	0.15	0.98	0.98	0.005	100	5.00E+08	0.961	1
LCZ F: Bare soil or sand	0.2	0.15	0.98	0.98	0.005	100	5.00E+08	0.961	0
LCZ G: Water	0	0.05	0	0.99	0.0002	0	0	0	0

difference at nightfall are retained. The second term is related to erroneous simulations by UrbClim on days characterized by unstable weather conditions, on these days the model on occasion simulates temperatures wrongly. The second condition is thus a second check, to filter out days on which no UHI is seen in the simulated data, but we would expect one based on the regional weather prediction.

2.4.2. Thermal characteristics of mapped LCZs in Belgian study areas

The assessment of air temperature, based on the mapped LCZs in the three study sites, was done using simulated air temperature, provided at a spatial resolution of 100 m. For Antwerp, Brussels and Ghent, night-time (1 am local time) simulations in the modelling interval (summer periods 2014 and 2015) were selected to evaluate the thermal characteristics. Based on the modelling output for Antwerp, Brussels and Gent, 82, 101 and 76 nights were retained, respectively, as these nights displayed a clear UHI (see above). To verify the unique temperature regime linked to each zone (Stewart et al., 2014) the temperature regime of each individual zone was evaluated by plotting the distribution of simulated night-time air temperatures. To conform to the model assessment, raster values were normalized and statistical tests were performed to determine significant differences between the different zones. For each zone, the average air temperature anomaly from the average overall air temperature was calculated and inter-LCZ temperature distributions and their differences were assessed.

2.4.3. Influence of LCZs on heat stress in the Belgian study areas

To relate our findings to information relevant to urban planners or policy makers, we assess whether the impact of a heatwave is different across different LCZs. In Belgium, a heatwave is defined as a consecutive 5-day period with maximum temperatures above 25 °C during which at least three days have maximum temperatures higher than 30 °C (Brouwers et al., 2015). It is important to note that in addition to extremely high daytime temperatures, high nocturnal temperatures that have negative health consequences are also important for the development of heat stress situations (Wouters et al., 2017). For this reason, the Belgian Federal Government Bureau of Public Health developed a different standard for heatwaves incorporating daily minimum temperatures. According to the Bureau, a heatwave is defined as any consecutive 3-day period where the mean maximum and mean minimum temperatures are higher than 29.6 °C and 18.2 °C, respectively, over a period of at least three consecutive days (Wouters et al., 2017). Based on the latter definition the Flemish Environmental Agency (Vlaamse Milieu Maatschappij; VMM) has constructed a heat stress indicator known as the Heatwave Degree Days (HDD) (Brouwers et al., 2015), defined as:

$$HDD = \sum_{k} [(T_{min,k} - 18.2\ ^{\circ}C)^{+} + (T_{max,k} - 29.6\ ^{\circ}C)^{+}]h_k$$

This index calculates the sum of exceedance of minimum and maximum thresholds during a heatwave day ($h_k = 1$). The intensity of the heatwaves is taken into account with the concept of exceeding values of those temperature thresholds. The plus sign, $()^{+}$, indicates that only positive values are taken into account. This index allows for the assessment of the magnitude of the heatwave in different places or the impact of a heatwave in different local climate zones.

3. Results

3.1. Assessment of the UrbClim model based on Augsburg data

The performance of the UrbClim model is assessed over Augsburg by comparing the simulated to the observed air temperature, stratified by LCZ class. Fig. 6 depicts a clear decrease in night-time air temperature when LCZs become more open and vegetated, for example, LCZ 5 and LCZ 6. The compact midrise class (LCZ 2) is the hottest zone. This is not only apparent in the observations, but also from the UrbClim results.

Fig. 5. A sub-set of observation locations in Augsburg.

The statistical *t*-test confirms that all built zones with the exception of LCZ 5 versus LCZ 8 experience significantly different thermal behavior for both the observed and the simulated temperature data. In Fig. 7, we see a clear overestimation of the night-time temperature for the whole study area by 2 °C.

Given these results, we further compared the results from the validated model runs for Brussels and the simulations generated in this study. While we focused only on Brussels in July 2014, similar results were found for the other cities and other dates. We compared the time series of the mean temperature over the entire study area of Brussels for both runs. The difference between the mean temperature over the domain in the validated runs and the one in LCZ runs is always rather small, especially in comparison with the RMSE-values typically observed in validations of the UrbClim model (Lauwaet et al., 2016). Second, we considered the gridded mean temperature over July 2014 (Fig. A2). Both the scatterplot and the statistics indicated at a good comparison between both data sets: the bias and RMSE were much smaller than the errors on the UrbClim results. Given these results, we have confidence in the use of the simulation results from the UrbClim model for Antwerp, Brussels, and Ghent for the remainder of this manuscript.

3.2. Thermal characteristics of LCZs in the Belgian study areas

A next step is the assessment of the simulated night-time air temperature for Antwerp, Brussels and Ghent (Figs. 8 and 9). The boxplots in Fig. 8 show similar features to the ones displayed for Augsburg, namely that open (vegetated zones) are relatively cooler than compact zones. Fig. 9 depicts the absolute air temperature, as the anomaly from the domain mean and the inter-LCZ differences. For all our study areas, the hottest zones are the compact built zones (LCZ 2 & LCZ 3), followed by all zones linked to industrial functions (LCZ 8, LCZ 10, and LCZ E). A significant drop in temperature is observed between compact lowrise (LCZ 3) and open lowrise (LCZ 6), and between open lowrise (LCZ 6) and sparsely built (LCZ 9). This temperature drop corresponds to the increase in vegetation cover and the higher sky view factors. Also in the natural zones (LCZs A, B, D & G) large differences can be found in the thermal characteristics of the different zones. The high heat capacity of

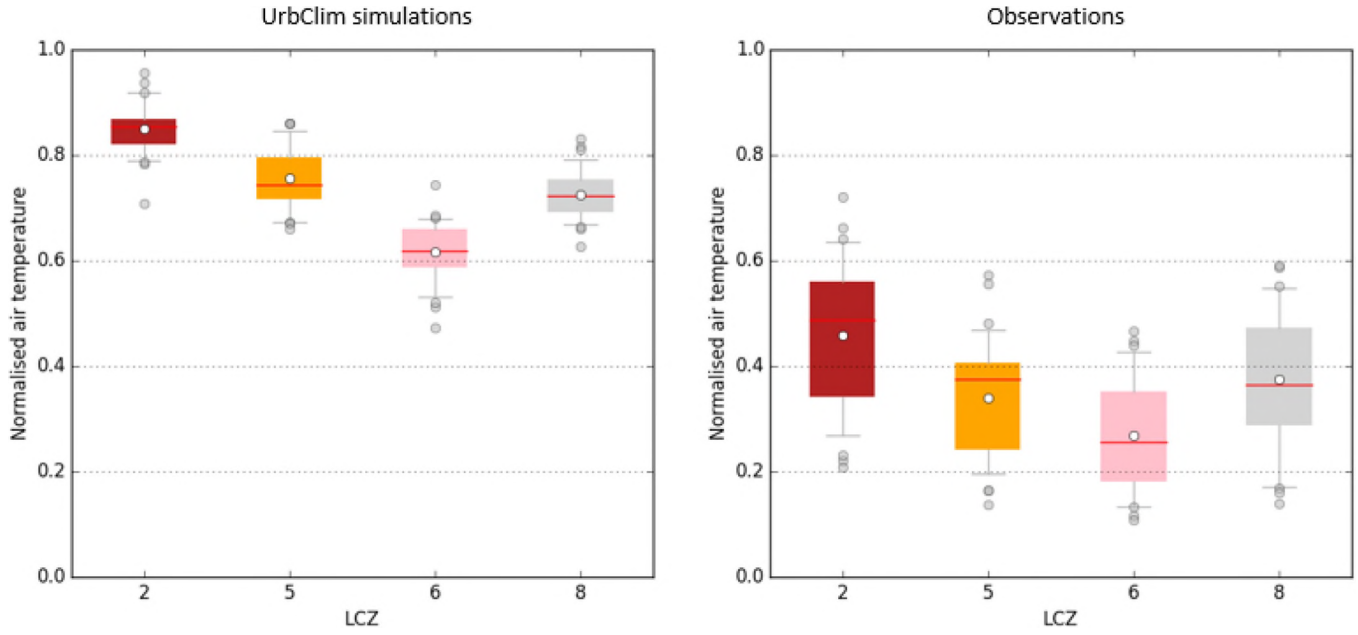

Fig. 6. Boxplots of the normalised temperature in different LCZs in Augsburg, based on the mean temperature of a zone at 1 am for the UrbClim simulations (left) and based on the mean of the temperature at 1 am at the different observation locations for a zone (right). Y axis: the normalised temperature; the X axis: the different zones; median temperature: red stripe; average air temperature: white dot; boxplot ends: first and third quantile; horizontal stipes: +/− the 1.5 fold interquartile range on air temperature values and outliers: grey dots. (For interpretation of the references to colour in this figure legend, the reader is referred to the web version of this article.)

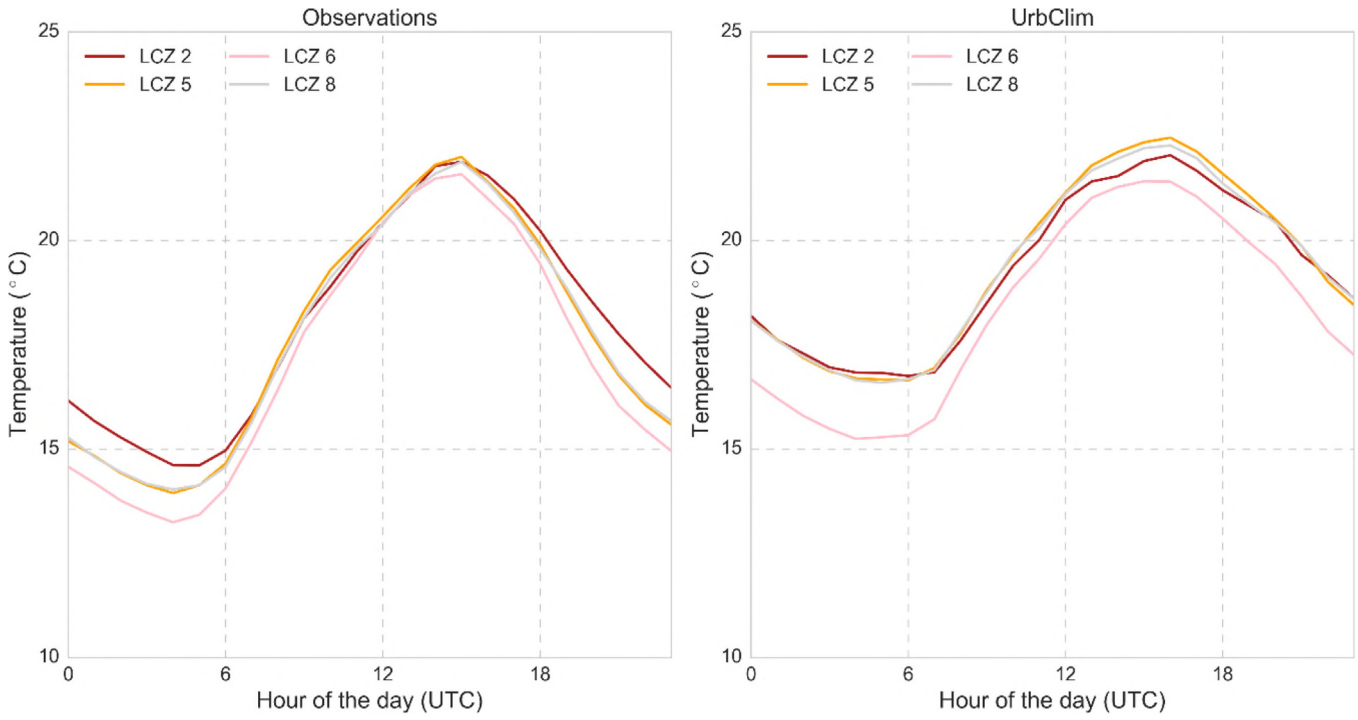

Fig. 7. Mean diurnal cycle for logger data and UrbClim simulations for the city of Augsburg. The hourly mean temperature values are derived from all valid logger observations between June 1st and September 30th of the years 2014 and 2015 (5585 hourly timesteps). For UrbClim, the corresponding valid time steps are taken.

water (LCZ G) results in a reduced night-time cooling effect, which creates natural hot-spots during the night (Broadbent, Tapper, Coutts, & Demuzere, 2017). Scattered trees (LCZ B) and low plants (LCZ D) are again much cooler.

For Antwerp (Fig. 9a, b), the hottest zone is on average, 1.5 °C hotter at night compared to the average air temperature in all zones. All natural zones except for water are 0.5 to almost 2 °C cooler than the average air temperature. Overall, we thus observe an average UHI intensity for the city of Antwerp of 2.8 ± 1.0 °C. Maximum UHI intensities, however, can go up to almost 6.5 °C. The difference between the hottest and the coolest built zone already accounts for a large part of this intensity. Fig. 9b shows that when temperature differences are large, the standard deviation of the mean temperature difference between zones is large as well. Statistical analysis also shows that all zones in Antwerp have significantly different thermal characteristics except for the industrial zones: large lowrise (LCZ 8) and heavy industry

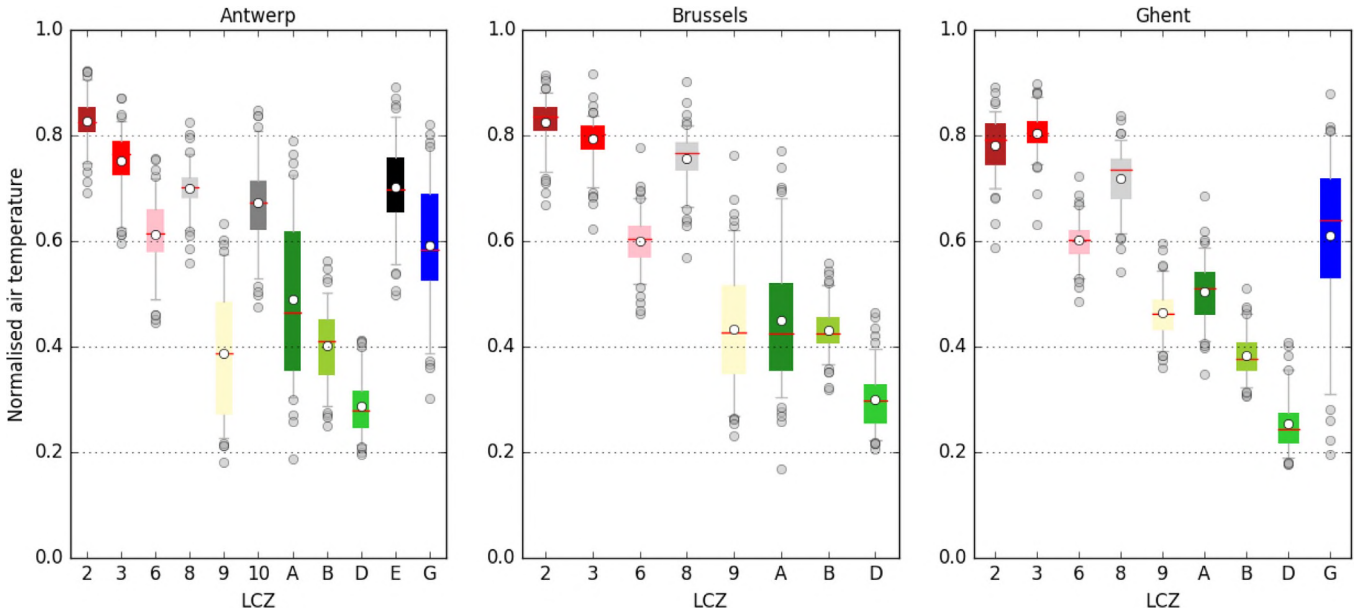

Fig. 8. Boxplots of the normalised temperature in different LCZs based on the mean temperature of a zone at 1 am for the UrbClim simulations for Antwerp, Brussels and Ghent. Y axis: the normalised temperature; the X axis: the different zones; median temperature: red stripe; average air temperature: white dot; boxplot ends: first and third quantile; +/− the 1.5 fold interquartile range on air temperature values: horizontal stripes and outliers: grey dots. (For interpretation of the references to colour in this figure legend, the reader is referred to the web version of this article.)

(LCZ 10) (Fig. 9b).

Similar results are found for the city of Brussels (Fig. 9c, d). The natural zones and the sparsely built zone are all at least 0.5 °C cooler than the average night-time temperature in Brussels. The overall UHI intensity amounts to 2.9 ± 0.7 °C on average but the boxplot indicates that the range was quite large with maximum UHI intensities exceeding 5 °C.

Ghent shows some dissimilarity with Antwerp and Brussels. The warmest zone is compact lowrise (LCZ 3) (Fig. 8). The difference with compact midrise (LCZ 2) is, however, smaller (0.2 ± 0.3 °C) than the uncertainty range. Within these error margins, no significant difference can thus be observed. The coolest zones are between 0.4 °C and almost 2 °C cooler than the average night-time air temperature (Fig. 9e, f). Water is slightly warmer than the average night-time air temperature. Overall, we observe a UHI intensity of 3.3 ± 0.8 °C. Maximum UHI intensity reached nearly 6 °C on the hottest nights (Fig. 9f). Ranges of the overall UHI intensity and the temperature difference between the hottest and the coolest LCZ are large, as was the case for Antwerp and Brussels.

3.3. Analysis of the influence of LCZs on heat stress

Information on relative and absolute temperature differences does not provide information on areas that are more prone to heat stress. To assess the exposure to heat in the mapped LCZs, the thresholds for maximum (day-time) and minimum (night-time) air temperature values for Belgium are used (Wouters et al., 2017).

In Fig. 10, the results for the HDD are shown. Compact built zones (LCZ 2 and LCZ 3) were subject to most distinct heat stress in the three cities and because these densely built zones contain a large proportion of the population, a significant number of people are thus affected by the heat. In Antwerp, industrial zones (LCZ 10 and LCZ E) also featured considerable heat stress. However, the impact at night will be smaller because these regions are mostly located outside of residential zones.

In Figs. A3–A5 (a) the thresholds are plotted along with the maximum and minimum air temperature for each day in each LCZ during the summer months in 2014. It is apparent that a heatwave occurred in the second half of July. For this period, the graph is enlarged to highlight the effects of maximum (b) and minimum (c) air temperature for the different LCZs.

For Antwerp (Fig. A3), it is clear that all zones exceeded the thresholds for maximum and minimum temperature, respectively, from the 17th until the 20th of July and from the 18th until the 20th of July. Some of the zones cooled much faster relative to others. For example, at day-time, low plants (LCZ D) had the second highest maximum temperature during the heatwave, whereas at night, the zone cooled down to the lowest values zone. While the compact mid-rise (LCZ 2) did not exceed the maximum threshold, it exceed the minimum threshold. During the day, all zones became hot and the differences in temperature were rather small. Excluding dense trees (LCZ A), temperature differences between the zones were smaller than 2 °C during the day. At night, however, temperature differences were more pronounced and rose to 4 °C. During the day the coolest zones were water (LCZ G) and dense trees (LCZ A); at night zones low plants (LCZ D) and scattered trees (LCZ B) were the coolest. It is also apparent that on the 21st of July, there was a steep decrease in temperature, as all zones went below the minimum threshold on that night except for compact midrise (LZC 2).

Similar phenomena are shown for Brussels and Ghent (Figs. A4 and A5). However, temperature differences during day-time and night-time were smaller, about 1 °C and 3 °C, respectively, for both cities. In both study zones, minimum temperatures decreased below the threshold value during the temperature drop on the 21st of July.

4. Discussion

A first step was the evaluation of the UrbClim model. From the comparison between the validated model runs and the simulations based on LCZs (Fig. A2), we can conclude that UrbClim represents the overall observed temperature in the modelling domain, but not that the model is able to thermally distinguish between the different urban local climate zones. Therefore, the modelling results from the UrbClim model using LCZ maps have been compared to a unique set of observations from the city of Augsburg to evaluate the modelling performance in the different urban LCZs. Fig. 7 shows that there was an overall overestimation of the modelled ambient night-time air temperature of approximately 2 °C. Even though we do not see this effect in the Belgian study areas (Fig. A2), a similar effect was

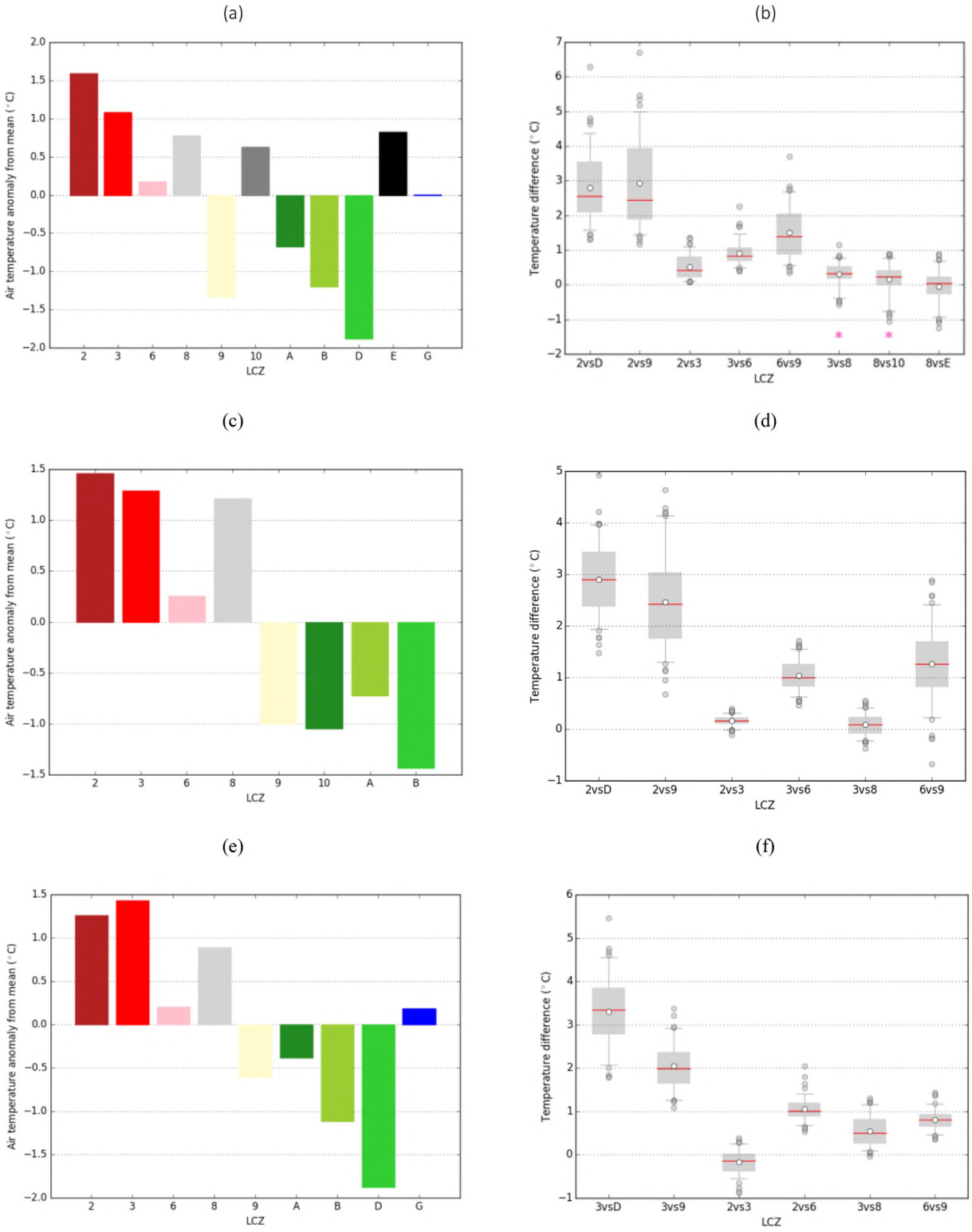

Fig. 9. Temperature differences between LCZs in a bar chart representing the average night-time air temperature anomaly for each LCZ from the average night-time air temperature, boxplots representing the absolute air temperature differences between two different LCZs. Antwerp (a) and (b), Brussels (c) and (d), Ghent (e) and (f). Median temperature: red stripe; average air temperature: white dot; boxplot ends: first and third quantile; +/− the 1.5 fold interquartile range on air temperature values: horizontal stripes and outliers: grey dots; *(fuchsia) insignificant thermal difference between zones. (For interpretation of the references to colour in this figure legend, the reader is referred to the web version of this article.)

seen in Barcelona, where it is a consequence of the underestimation of the sea breeze by the ERA-intrim data (García-Díez et al., 2016). In the case of our Belgian study cities, it is most likely an overestimation due to winds coming from the Alps. Regardless, for this study the main importance of the Augsburg analysis is the comparison of thermal patterns in the built zones, which are based on normalized night-time air temperatures. The results here showed that even though the UrbClim model generated slightly different outputs, the simulated temperatures for the built zones followed the

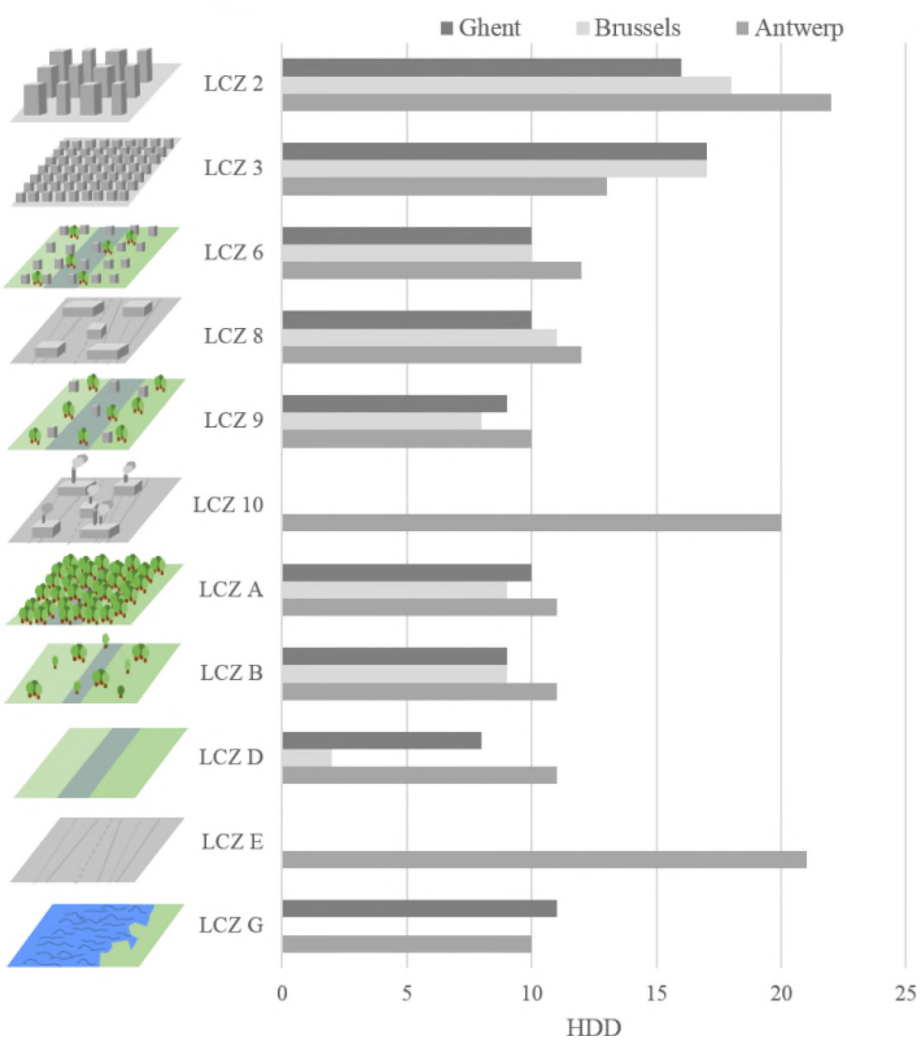

Fig. 10. Heatwave degree days (HDD) for different LCZs in Antwerp, Brussels and Ghent.

patterns shown by the ambient air temperature data from the observations. It is apparent, however, that the boxplots for the observed temperature data have a wider range and have relatively lower values than the ones for the UrbClim simulations. It should be taken into account that the observed temperature data represents the mean value of a number of points (loggers) in the zone, whereas the simulated data is evaluated as the mean value for the whole zone. A closer evaluation of the observed temperatures shows that often one or more loggers in a specific LCZ record higher temperatures than the other loggers in the same zone. Due to the applied normalization, this can lead to the relatively low boxplot values and the wide ranges on these values for the logger data compared to the simulated data. Based on these results and the comparison to the validated model runs for our selected study sites, we are confident in the UrbClim simulations for the Belgian cities in this study.

In the second part of this work, we investigated the LCZ thermal characteristics based on simulated temperature data. First, we verified whether all the zones in the three cities were thermally different, as was indicated by (Stewart et al., 2014). Second, thermal differences were quantified and evaluated. Our results add to the growing body of literature on the thermal behavior of LCZs (Alexander & Mills, 2014; Fenner et al., 2017; Holmer et al., 2013; Kotharkar & Bagade, 2018; Leconte et al., 2017; Lehnert et al., 2014; Ndetto & Matzarakis, 2015; Puliafito et al., 2013; Skarbit et al., 2017; Thomas et al., 2014; Villadiego & Velay-Dabat, 2014), providing evidence that the LCZ maps can be used to reasonably simulate intra-urban air temperature differences in cities. Since we studied three different cities, we argue that the LCZ maps can be used as an indication for hotter and cooler zones in urban areas independent of the city.

The importance of the temperature difference becomes especially clear when the HDDs are taken into account. Unlike information on heat stress, simply knowing whether zones are hotter or cooler will not provide urban planners with information on which areas to target in the future. In the compact zones, heat stress during heatwaves was much higher compared to the other zones. This is illustrated in Fig. 10, which depicts how the more vegetated and open zones cool down below the heatwave threshold during the night and provide a recovery period for its inhabitants. Recent work by Wouters et al. (2017), confirms the need for targeted mitigation measures in urban areas. According to their simulations, heat stress in urban centers in Belgium will rise by a factor 1.4 to 15 depending on the greenhouse gas emissions and land use change scenario. The fact that the LCZ scheme appears to be useful in urban climate models opens a plethora of possibilities for future work, for instance, urban planning scenarios can be evaluated using models, which can predict the thermal behavior of the planned zones under climate change conditions. Urban planners can use these scenarios to account for areas that are more prone to suffer from heat stress. When data on vulnerability and exposure (age groups, income status, obesity rates, distance and access to cool spots for each neighborhood) are available, the potential of the LCZ maps could be extended to serve as a tool for heat risk analysis. For example, the inhabitants of the “Rabot” neighborhood in Ghent live in an area with the highest population density in the city, where median income is among the lowest, unemployment rates are high and access to green spaces is limited (Stad Gent, 2017). On the other hand, the

neighborhood “Stationsbuurt-Noord”, which suffers from the same amount of HDDs, has lower population densities and unemployment rates but enjoys higher incomes and access to green space. Following the “Crichton’s Risk Triangle” (Crichton, 1999), the combination of high hazard, exposure and vulnerability make that the inhabitants of the “Rabot” neighborhood are potentially more prone to suffer from heat stress than the inhabitants of “Stationsbuurt-Noord”. However, the LCZ maps only provide input on weather hazard, not on vulnerability and exposure of the population. The LCZ maps can thus not be interpreted as heat risk maps but instead have the potential to serve as an indicator for heat stress. This is important knowledge for urban planners, as knowing where the need for adaptive or mitigation measures is highest can assist in informed decision-making. This was recently acknowledged by the IPCC in the concluding remarks at the Cities and Climate Change Science Conference in Edmonton (IPCC, 2018): “There is a need for easy-to-use assessment tools for urban planners”.

Since we are working with a secondary product of the LCZ scheme, we would like to stress the need for highly accurate maps supported by an extensive accuracy assessment (Verdonck et al., 2017) when using the maps as an indicator for heat stress. Furthermore, we also want to emphasize that we studied three different cities in this study, which all confirm that LCZ maps can be used as an indicator for heat stress. Overall, these results show the robustness of the maps as a powerful tool for urban planners.

5. Conclusion

The overall aim of this paper was to verify whether LCZ maps have value in differentiating air temperatures using simulated data from an urban climate model and analyze LCZ maps as an objective indicator for heat stress in cities.

By using the unique observation dataset, we were able to confirm the model results and provide evidence for the use of LCZ maps as a heat stress indicator. These results further support the mapping scheme as an indispensable tool for future urban planning and confirm the thermal differentiation between the different LCZs based on the unique observation dataset as well as modelled air temperature. Densely built zones were significantly warmer compared to more open and vegetated zones. It was also shown that even though thermal differences between the built zones might be small, the cooling rate in night-time temperatures can be large, and that this cooling at night is often crucial in terms of human health. The population in densely built zones are thus more likely to be affected by heat stress.

Since current trends show a population increase in dense urban areas (WMO, 2013), these zones should get more attention by urban planners worldwide. When available, knowledge of thermal behavior of cities is generally difficult to gather for more than a few spots or its quality cannot be verified (crowdsourced data). Currently, over 90 cities worldwide along with two important city networks, C40 and ICLEI, have expressed interest in spatially resolved LCZ maps (WUDAPT, n.d.) to study their respective urban climates. This study can thus contribute to research on urban climate globally.

Acknowledgements

This work is funded by the Belgian Federal Science Policy Office, as part of the UrbanEARS project. We would also like to thank Travis W. Drake for proofreading the manuscript.

Appendix

See Figs. A1–A5.

	F1-score							
OA	LCZ 2	LCZ 5	LCZ 6	LCZ 8	LCZ A	LCZ B	LCZ D	LCZ G
92.8	87.8	75.5	90.2	94.4	98.3	72.0	97.4	100

Fig. A1. Confusion matrix for LCZ map Augsburg.

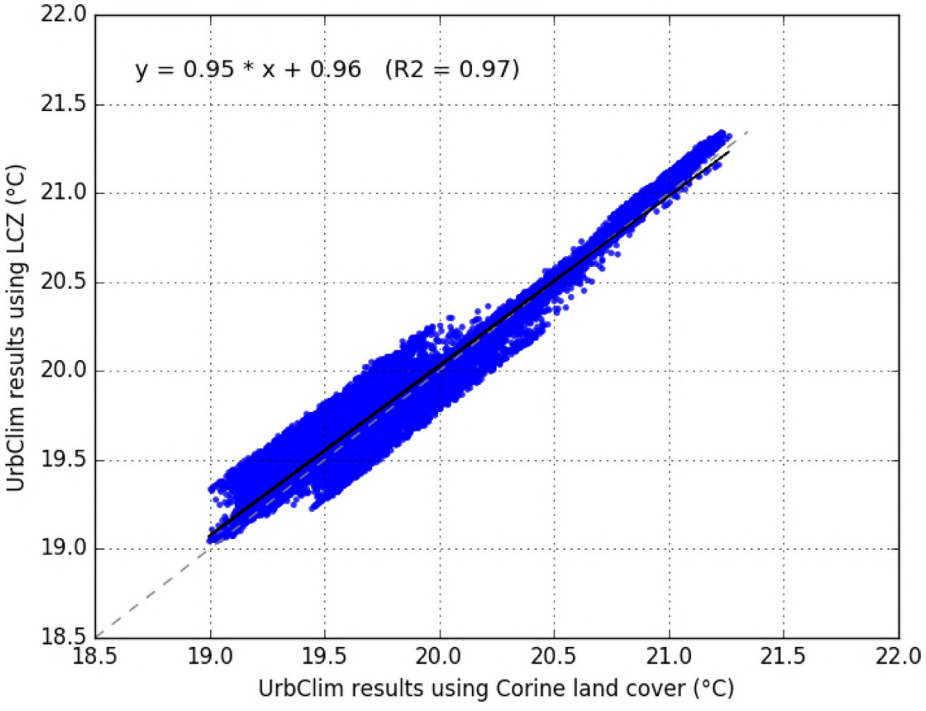

Fig. A2. Scatterplot of the temperatures obtained using the LCZ-map as a function of the temperature of the same grid cell when the CORINE-map is used for the city of Brussels. The black line indicates the least square linear fit, and the dashed line indicates the 1-to-1 relation. Difference statistics, for the mean gridded temperatures for the city of Brussels are: Bias (°C): 0.12, RMSE (°C): 0.17, Pearson R: 0.98, Linear coefficient of fit: 0.92. A positive bias refers to a higher mean temperature for the LCZ-map.

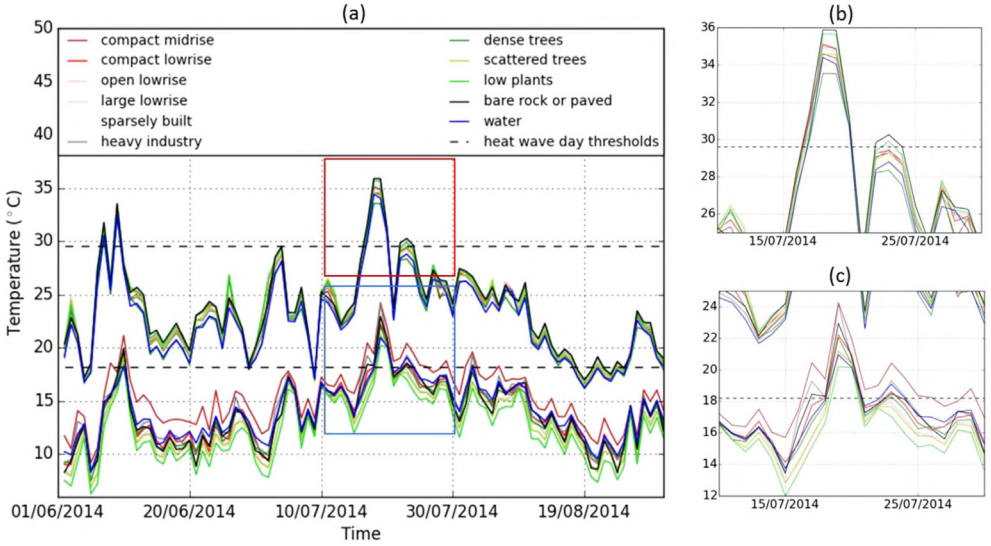

Fig. A3. (a) Maximum and minimum temperature plots for the summer days (June-August) in 2014 for Antwerp (b) zoom in on maximum temperature during heatwave and (c) zoom in on minimum temperature during heatwave.

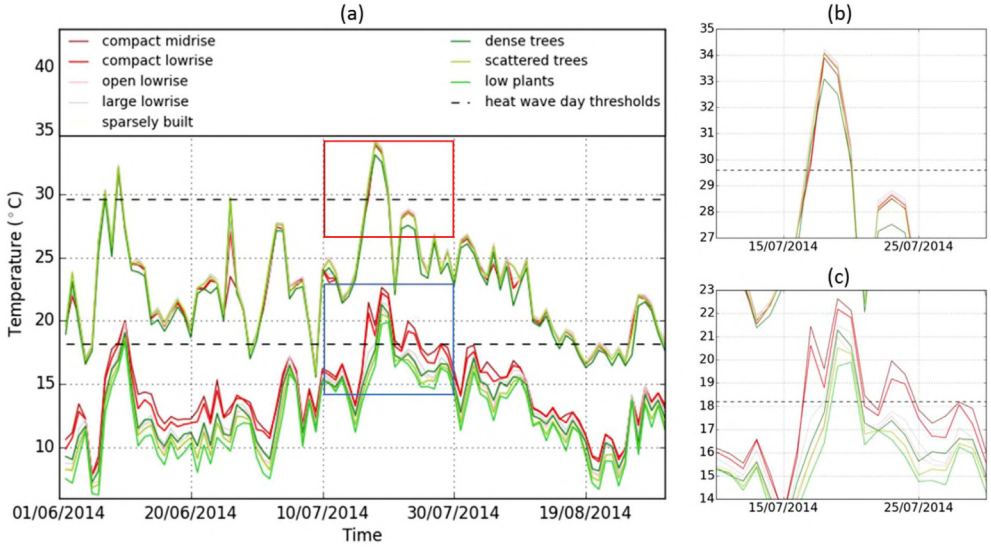

Fig. A4. (a) Maximum and minimum temperature plots for the summer days (June-August) in 2014 for Brussels (b) zoom in on maximum temperature during heatwave and (c) zoom in on minimum temperature during heatwave.

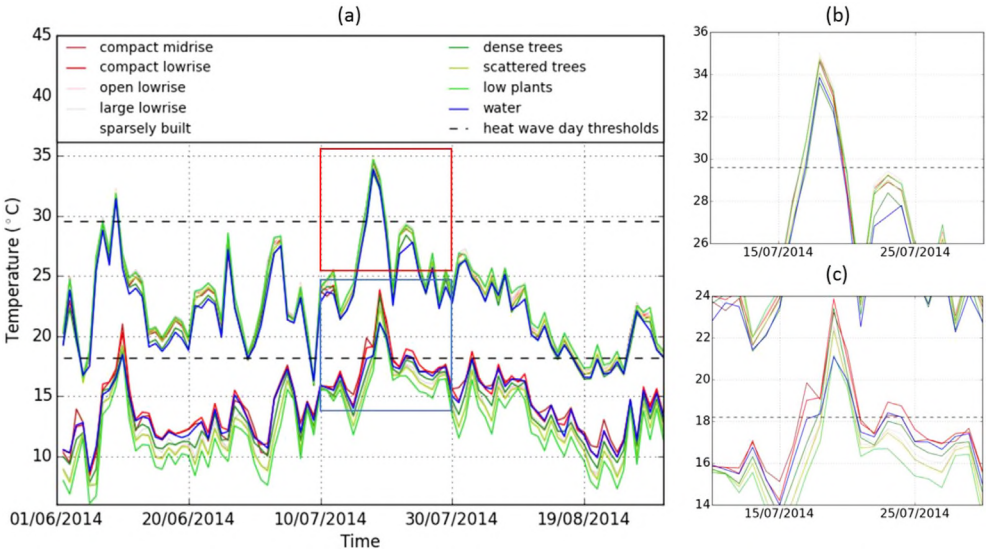

Fig. A5. (a) Maximum and minimum temperature plots for the summer days (June-August) in 2014 for Ghent (b) zoom in on maximum temperature during heatwave and (c) zoom in on minimum temperature during heatwave.

References

Aertsens, J., Nocker, L. de, Lauwers, H., Norga, K., Simoens, I., Meiresonne, L., Ellipsis Broekx, S. (2012). Daarom groen! Waarom u wint bij groen in uw stad of gemeente (That's why green! Why you gain with green in your city of town). Studie Uitgevoerd in Opdracht van: ANB – Afdeling Natuur En Bos, (November), 144 pp.

Alexander, P. J., Fealy, R., & Mills, G. M. (2016). Simulating the impact of urban development pathways on the local climate: A scenario-based analysis in the greater Dublin region, Ireland. *Landscape and Urban Planning, 152*, 72–89. http://dx.doi.org/10.1016/j.landurbplan.2016.02.006.

Alexander, P. J., & Mills, G. (2014). Local climate classification and Dublin's urban heat island. *Atmosphere, 5*(4), 755–774. http://dx.doi.org/10.3390/atmos5040755.

Barriopedro, D., Fischer, E. M., Luterbacher, J., Trigo, R., & Garcia-Herrera, R. (2011). The hot summer of 2010: Redrawing the temperature record map of Europe. *Science, 332*(6026), 220–224.

Bechtel, B., Alexander, P., Böhner, J., Ching, J., Conrad, O., Feddema, J., ... Stewart, I. (2015). Mapping local climate zones for a worldwide database of the form and function of cities. *ISPRS International Journal of Geo-Information, 4*(1), 199–219. http://dx.doi.org/10.3390/ijgi4010199.

Bechtel, B., Demuzere, M., Sismanidis, P., Fenner, D., Brousse, O., Beck, C., ... Verdonck, M. L. (2017). Quality of crowdsourced data on urban morphology – The human influence experiment (HUMINEX). *Urban Science, 1–21*. http://dx.doi.org/10.3390/urbansci1020015.

Beck, C., Breitner, S., Cyrys, J., Hald, C., Hartz, U., Jacobeit, J., ... Wolf, K. (2015). Statistical modeling of urban air temperature distributions under different synoptic conditions. *Geophysical Research Abstracts, 17*, 2015 EGU2015-15292.

Best, M. J., & Grimmond, C. S. B. (2015). Key conclusions of the first international urban land surface model comparison project. *Bulletin of the American Meteorological Society, 96*(5), 805–819. http://dx.doi.org/10.1175/BAMS-D-14-00122.1.

Bowler, D. E., Buyung-Ali, L., Knight, T. M., & Pullin, A. S. (2010). Urban greening to cool towns and cities: A systematic review of the empirical evidence. *Landscape and Urban Planning, 97*(3), 147–155. http://dx.doi.org/10.1016/j.landurbplan.2010.05.006.

Broadbent, A. M., Tapper, N. J., Coutts, A. M., & Demuzere, M. (2017). The cooling effect of irrigation on urban microclimate during heatwave conditions. *Urban Climate*. http://dx.doi.org/10.1016/j.uclim.2017.05.002 Special Is.

Brousse, O., Martilli, A., Foley, M., Mills, G., & Bechtel, B. (2016). WUDAPT, an efficient land use producing data tool for mesoscale models? Integration of urban LCZ in WRF over Madrid. *Urban Climate, 17*, 116–134. http://dx.doi.org/10.1016/j.uclim.2016.04.001.

Brouwers, J., Peeters, B., Van Steertegem, M., Van Lipzig, N., Wouters, H., Beullens, J., … Cauwenberghs, K. (2015). MIRA climate report 2015: About observed and future climate changes in flanders and Belgium.

Champeaux, J. L., Masson, V., & Chauvin, F. (2005). ECOCLIMAP: A global database of land surface parameters at 1 km resolution. *Meteorological Applications, 12*(1), 29–32. http://dx.doi.org/10.1017/S1350482705001519.

Ching, J., Mills, G., Bechtel, B., See, L., Feddema, J., Wang, X., ... Theeuwes, N. (2018). 0: World Urban Database and Access Portal Tools (WUDAPT), an urban weather, climate and environmental modeling infrastructure for the Anthropocene. *Bulletin of the American Meteorological Society* 0, http://dx.doi.org/10.1175/BAMS-D-16-0236.1.

Coutts, A. M., Tapper, N. J., Beringer, J., Loughnan, M., & Demuzere, M. (2012). Watering our cities: The capacity for Water Sensitive Urban Design to support urban cooling and improve human thermal comfort in the Australian context. *Progress in Physical Geography, 37*(1), 2–28. http://dx.doi.org/10.1177/0309133312461032.

Crichton, D. (1999). The risk triangle. In J. Ingleton (Ed.). *Natural disaster management* (pp. 102–103). London: Tudor Rose.

Danielson, J. J., Gesch, D. B. (2011). Global multi-resolution terrain elevation data 2010. US Department of the Interior and US Geological Survey (2011). US Department of the Interior and US Geological Survey.

De Ridder, K. (2006). Testing Brutsaert's temperature roughness parameterization for representing urban surfaces in atmospheric models. *Geophysical Research Letters, 33*(13), 12–15. http://dx.doi.org/10.1029/2006GL026572.

De Ridder, K., Lauwaet, D., & Maiheu, B. (2015). UrbClim – A fast urban boundary layer climate model. *Urban Climate, 12*, 21–48. http://dx.doi.org/10.1016/j.uclim.2015.01.001.

De Ridder, K., & Schayes, G. (1997). The IAGL land surface model. *Journal of Applied Meteorology, 36*(2), 167–182. http://dx.doi.org/10.1175/1520-0450(1997)036<0167:TILSM>2.0.CO;2.

Dee, D. P., Uppala, S. M., Simmons, A. J., Berrisford, P., Poli, P., Kobayashi, S., ... Vitart, F. (2011). The ERA-Interim reanalysis: Configuration and performance of the data assimilation system. *Quarterly Journal of the Royal Meteorological Society, 137*(656), 553–597. http://dx.doi.org/10.1002/qj.828.

Demuzere, M., De Ridder, K., & Van Lipzig, N. (2008). Modeling the energy balance in Marseille: Sensitivity to roughness length parameterizations and thermal admittance. *Journal of Geophysical Research Atmospheres, 113*(16), 1–19. http://dx.doi.org/10.1029/2007JD009113.

Demuzere, M., Harshan, S., Järvi, L., Roth, M., Grimmond, C. S. B., Masson, V., ... Wouters, H. (2017). Impact of urban canopy models and external parameters on the modelled urban energy balance in a tropical city. *Quarterly Journal of the Royal Meteorological Society, 143*(704), 1581–1596. http://dx.doi.org/10.1002/qj.3028.

Demuzere, M., Orru, K., Heidrich, O., Olazabal, E., Geneletti, D., Orru, H. A., ... Faehnle, M. (2014). Mitigating and adapting to climate change: Multi-functional and multi-scale assessment of green urban infrastructure. *Journal of Environmental Management, 146*, 107–115. http://dx.doi.org/10.1016/j.jenvman.2014.07.025.

EEA. (1994). CORINE land cover – contents. CORINE land cover. Retrieved from http://www.eea.europa.eu/publications/COR0-landcover/page001.html.

EEA. (2012). Imperviousness 2012. Retrieved February 28, 2018, from https://land.copernicus.eu/pan-european/high-resolution-layers/imperviousness/imperviousness-2012?tab=metadata.

Faroux, S., Kaptué Tchuenté, A. T., Roujean, J.-L., Masson, V., Martin, E., & Le Moigne, P. (2013). ECOCLIMAP-II/Europe: A twofold database of ecosystems and surface parameters at 1 km resolution based on satellite information for use in land surface, meteorological and climate models. *Geoscientific Model Development, 6*(2), 563–582. http://dx.doi.org/10.5194/gmd-6-563-2013.

Fenner, D., Meier, F., Bechtel, B., Otto, M., & Scherer, D. (2017). Intra and inter "local climate zone" variability of air temperature as observed by crowdsourced citizen weather stations in Berlin, Germany. *Meteorologische Zeitschrift, 26*(5), 525–547. http://dx.doi.org/10.1127/metz/2017/0861.

Feyisa, G. L., Dons, K., & Meilby, H. (2014). Efficiency of parks in mitigating urban heat island effect: An example from Addis Ababa. *Landscape and Urban Planning, 123*, 87–95. http://dx.doi.org/10.1016/j.landurbplan.2013.12.008.

García-Díez, M., Lauwaet, D., Hooyberghs, H., Ballester, J., De Ridder, K., & Rodó, X. (2016). Advantages of using a fast urban boundary layer model as compared to a full mesoscale model to simulate the urban heat island of Barcelona. *Geoscientific Model Development, 9*(12), 4439–4450. http://dx.doi.org/10.5194/gmd-9-4439-2016.

Grimm, N. B., Faeth, S. H., Golubiewski, N. E., Redman, C. L., Wu, J., Bai, X., & Briggs, J. M. (2008). Global change and the ecology of cities. *Science, 319*, 756–760.

Grimmond, C. S. B., Blackett, M., Best, M. J., Baik, J.-J., Belcher, S. E., Beringer, J., ...

Zhang, N. (2011). Initial results from Phase 2 of the international urban energy balance model comparison. *International Journal of Climatology, 31*(2), 244–272. http://dx.doi.org/10.1002/joc.2227.
Hammerberg, K., Brousse, O., Martilli, A., & Mahdavi, A. (2018). Implications of employing detailed urban canopy parameters for mesoscale climate modelling: A comparison between WUDAPT and GIS databases over Vienna, Austria. *International Journal of Climatology, 38*(February), 1241–1257. http://dx.doi.org/10.1002/joc.5447.
Heldens, W., Taubenböck, H., Esch, T., Heiden, U., Wurm, M. (2013). Analysis of surface thermal patterns in relation to urban structure types: A case study in Munich. In *Thermal infrared remote sensing* (pp. 475–493). Springer.
Hoag, H. (2015). How cities can beat the heat. *Nature, 524*, 402–404.
Holmer, B., Thorsson, S., & Lindén, J. (2013). Evening evapotranspirative cooling in relation to vegetation and urban geometry in the city of Ouagadougou, Burkina Faso. *International Journal of Climatology, 33*(15), 3089–3105. http://dx.doi.org/10.1002/joc.3561.
IPCC. (2018). Cities and Climate Change Science Conference.
Jackson, T. L., Feddema, J. J., Oleson, K. W., Bonan, G. B., & Bauer, J. T. (2010). Parameterization of urban characteristics for global climate modeling. *Annals of the Association of American Geographers, 100*(4), 848–865. http://dx.doi.org/10.1080/00045608.2010.497328.
Jain, S. P., & Rao, K. R. (1974). Experimental study on the effect of roof spray cooling on unconditioned and conditioned buildings. *Building Science, 9*(1), 9–16.
Kikegawa, Y., Genchi, Y., Kondo, H., & Hanaki, K. (2006). Impacts of city-block-scale countermeasures against urban heat-island phenomena upon a building's energy-consumption for air-conditioning. *Applied Energy, 83*(6), 649–668. http://dx.doi.org/10.1016/j.apenergy.2005.06.001.
Kleerekoper, L., Van Esch, M., & Salcedo, T. B. (2012). How to make a city climate-proof, addressing the urban heat island effect. *Resources, Conservation and Recycling, 64*, 30–38. http://dx.doi.org/10.1016/j.resconrec.2011.06.004.
Koppe, C., Kovats, S., Jendritzky, G., Menne, B. (2004). *Heat-waves: Risks and responses*. *Health and Global Environmental Health Series* (Vol. No.2). Retrieved from http://www.euro.who.int/eprise/main/WHO/Progs/CASH/HeatCold/20040331_1.
Kotharkar, R., & Bagade, A. (2018). Evaluating urban heat island in the critical local climate zones of an Indian city. *Landscape and Urban Planning, 169*(June 2017), 92–104. http://dx.doi.org/10.1016/j.landurbplan.2017.08.009.
Lauwaet, D., De Ridder, K., Saeed, S., Brisson, E., Chatterjee, F., van Lipzig, N., ... Hooyberghs, H. (2016). Assessing the current and future urban heat island of Brussels. *Urban Climate, 15*, 1–15. http://dx.doi.org/10.1016/j.uclim.2015.11.008.
Lauwaet, D., Maiheu, B., Aertsens, J., & De Ridder, K. (2013). Opmaak van een hittekaart en analyse van het stedelijk hitte-eiland effect voor Antwerpen (Development of a heat map and analysis of the UHI-effect in Antwerp).
Lauwaet, D., Hooyberghs, H., Maiheu, B., Lefebvre, W., Driesen, G., Van Looy, S., & De Ridder, K. (2015). Detailed urban heat island projections for cities worldwide: Dynamical downscaling CMIP5 global climate models. *Climate, 3*(4), 391–415. http://dx.doi.org/10.3390/cli3020391.
Leconte, F., Bouyer, J., Claverie, R., & Pétrissans, M. (2017). Analysis of nocturnal air temperature in districts using mobile measurements and a cooling indicator. *Theoretical and Applied Climatology, 130*(1–2), 365–376. http://dx.doi.org/10.1007/s00704-016-1886-7.
Lehnert, M., Geletič, J., Husák, J., & Vysoudil, M. (2014). Urban field classification by "local climate zones" in a medium-sized Central European city: The case of Olomouc (Czech Republic). *Theoretical and Applied Climatology, 122*(3–4), 531–541. http://dx.doi.org/10.1007/s00704-014-1309-6.
Lelieveld, J., Evans, J. S., Fnais, M., Giannadaki, D., & Pozzer, A. (2015). The contribution of outdoor air pollution sources to premature mortality on a global scale. *Nature, 525*, 367–371. http://dx.doi.org/10.1038/nature15371.
Maiheu, B., Van den Berghe, K., Boelens, L., De Ridder, K., Lauwaet, K. (2013). *Opmaak van een hittekaart en analyse van het stedelijk hitte-eiland effect voor Gent (Development of a heat map and analysis of the UHI-effect in Ghent)*.
Mills, G. (2007). Cities as agents of global change. *International Journal of Climatology, 27*(2007), 1849–1857.
Mirzaei, P. A. (2015). Recent challenges in modeling of urban heat island. *Sustainable Cities and Society, 19*, 200–206. http://dx.doi.org/10.1016/j.scs.2015.04.001.
Mora, C., Dousset, B., Caldwell, I. R., Powell, F. E., Geronimo, R. C., Bielecki, C. R., ... Trauernicht, C. (2017). Global risk of deadly heat. *Nature Climate Change, 7*, 501–506.
Ndetto, E. L., & Matzarakis, A. (2015). Urban atmospheric environment and human biometeorological studies in Dar es Salaam, Tanzania. *Air Quality, Atmosphere and Health, 8*(2), 175–191. http://dx.doi.org/10.1007/s11869-014-0261-z.
Oke, T. R. (1976). The distinction between canopy and boundary layer urban heat islands. *Atmosphere, 14*(February 2015), 268–277. http://dx.doi.org/10.1080/00046973.1976.9648422.
Onset. (2010). *HOBO ® Pro v2 (U23–00x) Manual Connecting the Logger*.
Papalexiou, S. M., AghaKouchak, A., Trenberth, K. E., & Foufoula-Georgiou, E. (2018). Global, regional, and megacity trends in the highest temperature of the year: Diagnostics and evidence for accelerating trends. *Earth's Future, 1–9*. http://dx.doi.org/10.1002/eft2.278.
Pickett, S. T. A., Cadenasso, M. L., & McGrath, B. (2013). *Resilience in ecology and urban design: Linking theory and practice for sustainable cities.* New York: Springer.
Puliafito, S. E., Bochaca, F. R., Allende, D. G., & Fernandez, R. P. (2013). Green areas and microscale thermal comfort in arid environments: A case study in Mendoza, Argentina. *Atmospheric and Climate Sciences, 3*(3), 372–384. http://dx.doi.org/10.4236/acs.2013.
Rizwan, A. M., Dennis, L. Y. C., & Liu, C. (2008). A review on the generation, determination and mitigation of Urban Heat Island. *Journal of Environmental Sciences, 20*(1), 120–128. http://dx.doi.org/10.1016/S1001-0742(08)60019-4.
Rosenfeld, A. H., Akbari, H., & Romm, J. J. (1998). Cool communities: Strategies for heat island mitigation and smog reduction. *Energy and Buildings, 28*, 51–62.
Salmond, J. A., Tadaki, M., Vardoulakis, S., Arbuthnott, K., Coutts, A., Demuzere, M., ... Wheeler, B. W. B. W. (2016). Health and climate related ecosystem services provided by street trees in the urban environment. *Journal of Environmental Health, 15*(S1), 1–40. http://dx.doi.org/10.1186/s12940-016-0103-6.
Schär, C., Vidale, P. L., Lüthi, D., Frei, C., Häberli, C., Liniger, M. A., & Appenzeller, C. (2004). The role of increasing temperature variability in European summer heatwaves. *Nature, 427*(6972), 332–336.
Shahmohamadi, P., Che-Ani, A. I., Maulud, K. N. A., Tawil, N. M., & Abdullah, N. A. G. (2011). The impact of anthropogenic heat on formation of urban heat island and energy consumption balance. *Urban Studies Research, 2011*, 1–9. http://dx.doi.org/10.1155/2011/497524.
Simon, R., Niiro, M., & Gwinn, R. (1993). Prior ischemic stress protects against experimental stroke. *Neuroscience Letters, 163*, 135–137.
Skarbit, N., Stewart, I. D., Unger, J., & Gál, T. (2017). Employing an urban meteorological network to monitor air temperature conditions in the "local climate zones" of Szeged, Hungary. *International Journal of Climatology, 37*(March), 582–596. http://dx.doi.org/10.1002/joc.5023.
Solberg, S., Hov, Søvde, A., Isaksen, I. S. A., Coddeville, P., De Backer, H., ... Uhse, K. (2008). European surface ozone in the extreme summer 2003. *Journal of Geophysical Research: Atmospheres, 113*, 1–16. http://dx.doi.org/10.1029/2007JD009098.
Stad Gent. (2017). Gent in cijfers. Retrieved April 24, 2018, from http://gent.buurtmonitor.be/.
Stewart, I. D., & Oke, T. R. (2012). Local climate zones for urban temperature studies. *Bulletin of the American Meteorological Society, 93*(12), 1879–1900. http://dx.doi.org/10.1175/BAMS-D-11-00019.1.
Stewart, I. D., Oke, T. R., & Krayenhoff, E. S. (2014). Evaluation of the "local climate zone" scheme using temperature observations and model simulations. *International Journal of Climatology, 34*(4), 1062–1080. http://dx.doi.org/10.1002/joc.3746.
Sun, R., & Chen, L. (2012). How can urban water bodies be designed for climate adaptation? *Landscape and Urban Planning, 105*(1), 27–33.
Sundborg, A. (1951). Climatological studies in Uppsala with special regard to the temperature conditions in the urban area. *Geographica*, 22.
Takebayashi, H., & Moriyama, M. (2007). Surface heat budget on green roof and high reflection roof for mitigation of urban heat island. *Building and Environment, 42*(8), 2971–2979. http://dx.doi.org/10.1016/j.buildenv.2006.06.017.
The World Bank. (2017). Urban population (% of total). Retrieved January 24, 2018, from http://data.worldbank.org/indicator/.
Thomas, G., Sherin, A. P., Ansar, S., & Zachariah, E. J. (2014). Analysis of urban heat island in Kochi, India, using a modified local climate zone classification. *Procedia Environmental Sciences, 21*, 3–13. http://dx.doi.org/10.1016/j.proenv.2014.09.002.
Toparlar, Y., Blocken, B., Maiheu, B., & van Heijst, G. J. F. (2017). A review on the CFD analysis of urban microclimate. *Renewable and Sustainable Energy Reviews, 80*(January), 1613–1640. http://dx.doi.org/10.1016/j.rser.2017.05.248.
UN. (2014). *World Urbanization Prospects: The 2014 revision, (ST/ESA/SER.A/366)*.
Urano, A., Ichinose, T., & Hanaki, K. (1999). Thermal environment simulation for three dimensional replacement of urban activity. *Journal of Wind Engineering and Industrial Aerodynamics, 81*(1–3), 197–210. http://dx.doi.org/10.1016/S0167-6105(99)00017-3.
Verdonck, M. L., Okujeni, A., van der Linden, S., Demuzere, M., De Wulf, R., & Van Coillie, F. (2017). Influence of neighbourhood information on "Local Climate Zone" mapping in heterogeneous cities. *International Journal of Applied Earth Observation and Geoinformation, 62*, 102–113. http://dx.doi.org/10.1016/j.jag.2017.05.017.
Villadiego, K., & Velay-Dabat, M. A. (2014). Outdoor thermal comfort in a hot and humid climate of Colombia: A field study in Barranquilla. *Building and Environment, 75*, 142–152. http://dx.doi.org/10.1016/j.buildenv.2014.01.017.
Weng, Q., Lu, D., & Schbring, J. (2004). Estimation of land surface temperature-vegetation abundance relationship for urban heat island studies. *Remote Sensing of Environment, 84*, 468–483.
Werder, J. (2010). Heat stress, (202), 9.
WMO. (2013). *The global climate 2001–2010: A decade of climate extremes summary report*.
Wouters, H., De Ridder, K., Poelmans, L., Willems, P., Brouwers, J., Hosseinzadehtalaei, P., ... Demuzere, M. (2017). Heat stress increase under climate change twice as large in cities as in rural areas: A study for a densely populated midlatitude maritime region. *Geophysical Research Letters, 44*(17), 8997–9007. http://dx.doi.org/10.1002/2017GL074889.
Wouters, H., Demuzere, M., Blahak, U., Fortuniak, K., Maiheu, B., Camps, J., … van Lipzig, N. P. M. (2016). Efficient urban canopy parametrization for atmospheric modelling: description and application with the COSMO-CLM model (version 5.0_clm6) for a Belgian Summer. *Geoscientific Model Development Discussions*, (April), 0–40. doi: 10.5194/gmd-2016-58.
WUDAPT. (n.d.). World Urban Data and Access Portal Tools. Retrieved May 29, 2017, from http://www.wudapt.org.
Yamamoto, Y. (2005). Measures to mitigate urban heat islands. *Environmental and Energy Research Unit. Quarterly Review, 18*, 65–83.